ELSEVIER

Contents lists available at ScienceDirect

Environmental Pollution

journal homepage: www.elsevier.com/locate/envpol





Pilot scale treatment of PFAS-contaminated groundwater in a subsurface flow constructed wetland−evaluating multiple plant species[★]

Oscar Liljeström ^{a,*} , Dahn Rosenquist ^b, Dan B. Kleja ^c, Anja Enell ^c, Lutz Ahrens ^a

- a Swedish University of Agricultural Sciences (SLU), Department of Aquatic Sciences and Assessment, P. O. Box 7050, SE-750 07, Uppsala, Sweden
- ^b Laqua Treatment AB, Siriusvägen 16, SE-296 92, Yngsjö, Sweden
- ^c Swedish Geotechnical Institute (SGI), Olaus Magnus Väg 35, SE-581 93, Linköping, Sweden

ARTICLE INFO

Keywords: PFAS Phytoremediation Constructed wetland Groundwater Landfill leachate Biochar

ABSTRACT

Groundwater contamination by per- and polyfluoroalkyl substances (PFAS) is an emerging threat to drinking water quality, highlighting the need for effective treatment solutions. This study investigated subsurface flow constructed wetlands for treating groundwater contaminated with PFAS. The wetlands used a peat, biochar, and lightweight expanded clay aggregate (LECA) filter substrate, planted with either tufted sedge (Carex elata), fiber hemp (Cannabis sativa Futura 75), or an intercropping of the two Salix clones S. Wilhelm and S. Loden. The experiment was conducted under field conditions in Sweden, during one growing season, using PFAScontaminated groundwater impacted by landfill leachate. The study showed accumulation of PFAS in all plant species and the peat and biochar part of the filter substrate, with short-chain PFAS and perfluoroalkyl carboxylates (PFCAs) dominating when considering the whole plants (57 % and 77 % of ΣPFAS, respectively) and longchain PFAS and perfluoroalkyl sulfonates (PFSAs) dominating in the peat and biochar filter substrate (77 % and 54 % of SPFAS, respectively). Sorption to the filter substrate was shown to be the primary mechanism for PFAS removal. The highest plant PFAS concentrations were found in leaves, followed by roots, for all species, There was a difference in the PFAS composition profile when comparing different plant tissues, with PFCAs dominating in leaves (84 % of ΣPFAS) and PFSAs dominating in roots (66 % of ΣPFAS). All plant species were determined to have an above-ground tissue/water phase concentrations >10/1 for C₃-PFCA (PFBA). This was also observed for C. sativa with C4- and C7-PFCAs (PFPeA, PFOA), and C4- and C5-PFSAs (PFBS, PFPeS), for C. elata with C8-PFSA (L-PFOS), and for S. Loden with PFPeA. \sum PFAS phytoextraction potential from landfill leachate-impacted groundwater (mg/ha yr) was estimated to be 940 \pm 670 for C. sativa, 390 \pm 310 for S. Loden, 330 \pm 160 for S. Wilhelm, and 160 \pm 56 for *C. elata*.

1. Introduction

Per- and polyfluoroalkyl substances (PFAS) are an anthropogenic class of fluorinated organic compounds that contain at least one perfluorinated carbon atom (OECD, 2021). Various PFAS have been, and are, produced for many applications, such as aqueous film-forming firefighting foams (AFFF), industrial lubricants, and nonstick coatings (Gaines, 2022). PFAS have also been linked to several adverse health effects, such as cancer (Barry et al., 2013), reduced immune response to vaccines (Stein et al., 2016), and increased cholesterol levels (Nelson et al., 2010). Due to their mobile and persistent nature (Brunn et al., 2023), PFAS are transported and retained in the environment, and found

in air, soil, water, wildlife, and humans (Brusseau, 2024; Rauert et al., 2018; Fenton et al., 2021; Kwok et al., 2015; Kelly et al., 2009). Thus, posing a potential hazard to human health and the environment (Sunderland et al., 2019; Beale et al., 2022). One transport pathway of concern is the infiltration of PFAS from landfill leachate into groundwater systems (Hepburn et al., 2019), causing risks to water quality, including drinking water (Sörengård et al., 2022). It is therefore critical that remediation methods for PFAS-contaminated groundwater and its contamination sources are developed.

The treatment options available for PFAS-contaminated ground-water can broadly be divided into *in situ* and *ex situ* approaches, where *in situ* approaches aim to separate, degrade, or immobilize PFAS in the

E-mail address: oscar.liljestrom@slu.se (O. Liljeström).

https://doi.org/10.1016/j.envpol.2025.127199

 $^{^{\}star}\,$ This paper has been recommended for acceptance by Dr Hefa Cheng.

^{*} Corresponding author.

aguifer, such as in situ sonication (Laramay and Crimi, 2020), or the introduction of immobilizing additives (Hale et al., 2017). In contrast, ex situ approaches aim to remove the water from the aquifer to be treated on-site or at a centralized treatment facility, so-called pump and treat (Birnstingl and Wilson, 2024). A possible method for both in situ and ex situ approaches is phytoremediation (Ferrario et al., 2022; Nassazzi et al., 2023). Phytoremediation has been used as a method for remediating areas from metals and various organic contaminants (Ali et al., 2013; Gan et al., 2009). The process can broadly be divided into phytoextraction, phytostabilization, and phytodegradation (Salt et al., 1998). Earlier research into plant uptake of PFAS focused on its accumulation in crops and mainly had a food safety perspective (Stahl et al., 2009; Wen et al., 2013; Krippner et al., 2014). These studies did, however, also show the phytoextraction potential for PFAS (Lesmeister et al., 2021). Recently, investigations have also started to be carried out concerning both phytoextraction and phytodegradation of PFAS (Ferrario et al., 2022; Greger, 2021). Plants used in these phytoremediation trials include willows (Salix spp) and fiber hemp (Cannabis sativa) (Nassazzi et al., 2023; Nason et al., 2024; Huff et al., 2020; Sharma et al., 2020). These plants are currently used for biomass production on an industrial scale (Zegada-Lizarazu et al., 2010), making them interesting also from a phytoremediation perspective, as they produce a lot of biomass in a short time and have logistics for management in place. The wetland genus of true sedge (Carex) is not commercially grown, except for garden decoration purposes (Walter et al., 2002). It has, however, still attracted interest from PFAS researchers with the potential to be used in e.g. constructed wetlands (Greger, 2021; Zhang et al., 2021a). Previous studies have shown PFAS uptake in floating wetlands where plants were placed on rafts in ponds, enabling them to sorb PFAS through their roots (Awad et al., 2022), or more traditional open surface constructed wetlands where PFAS is both taken up in plants planted along edges and bottom of the wetland as well as providing good hydrological conditions for the co-sedimentation of PFAS (Yin et al., 2017). There are also subsurface flow constructed wetlands where, instead of an open pond, water is passed through a filter substrate with plants on top, allowing their roots to perforate the subsurface flow (Ferrario et al., 2022; Xiao et al., 2023). Various wetland plants can be used for this application, with sweet flag (Acorus calamus) being a common choice (Ferrario et al., 2022; Xiao et al., 2023; Kang et al., 2023; Ma et al., 2023). The filter substrate often consists of gravel or sand, allowing for biofilm formation (Xiao et al., 2023; Lott et al., 2023). An interesting addition to a subsurface flow constructed wetland would be to use a carbon-rich filter substrate, since granular activated carbon (GAC) and biochar have proven effective at sorbing, especially long-chain PFAS (Askeland et al., 2020; Philip et al., 2017). Phytoextraction has contrastingly been found to work better for short-chain PFAS (Nassazzi et al., 2023). In studies investigating constructed wetlands for nutrient removal, incorporating biochar into the filter substrate at a proportion of 10-20 % v/v has also been shown to increase plant growth (Kasak et al., 2018; Li et al., 2019a). A combination of a carbon-rich filter substrate and growing wetland plants could be an efficient approach to deal with both longand short-chain PFAS. Using this kind of wetland system to treat PFAS-contaminated groundwater impacted by nearby landfill facilities is an area currently lacking research.

This study thus aimed to evaluate the onsite treatment of PFAS-contaminated groundwater, impacted by landfill leachate, using subsurface constructed wetlands on a pilot scale at a waste management facility in Sweden. The filter substrate consisted of a novel combination of biochar and peat for PFAS sorption with a lightweight expanded clay aggregate (LECA) to ensure hydraulic permeability. The tested plants included willow (*Salix* spp clones Wilhelm and Loden), fiber hemp (*C. sativa* Futura 75), and tufted sedge (*Carex elata*), none of which, to the best of our knowledge, have been previously used for PFAS treatment in a subsurface constructed wetland.

2. Materials and methods

2.1. Standards and chemicals

In total, 29 PFAS were analyzed including C₃-C₁₃ perfluoroalkyl carboxylates (PFCAs) (i.e. PFBA, PFPeA, PFHxA, PFHpA, PFOA, PFNA, PFDA, PFUnDA, PFDoDA, PFTrDA, PFTeDA), C4-C10 perfluoroalkyl sulfonates (PFSAs) (i.e. PFBS, PFPeS, PFHxS, PFHpS, PFOS, PFNS, PFDS), 4:2, 6:2, 8:2 fluorotelomer sulfonate (4:2 FTSA, 6:2 FTSA, 8:2 methylper-FTSA), perfluorooctanesulfonamide (FOSA), (MeFOSAA), fluorooctanesulfonamidoacetic acid ethvlperfluorooctanesulfonamidoacetic acid (Et-FOSAA), tetrafluoro-2-(heptafluoropropoxy)propanoic acid (HFPO-DA), dodecafluoro-3H-4,8-dioxanonanoic acid (NaDONA), 9-chlorohexadecafluoro-3-oxanonane-1- sulfonic acid (6:2 Cl-PFESA), 11-chloroeicosafluoro-3-oxaundecane-1sulfonate acid (8:2)Cl-PFESA) and perfluoro-4ethylcyclohexanesulfonate (PFECHS). Standards for PFHxS and PFOS were quantified for both linear and branched isomers (L-PFHxS, B-PFHxS, L-PFOS, B-PFOS), (Table S1 in Supporting Information (SI)). In addition, 19 isotopically labeled PFAS standards (IS) were included (13C₄-PFBA, 13C₅-PFPeA, 13C₅-PFHxA, 13C₄-PFHpA, 13C₈-PFOA, 13C₉-PFNA, ¹³C₆-PFDA, ¹³C₇-PFUnDA, ¹³C₂-PFDoDA, ¹³C₂-PFTeDA, ¹³C₃-PFBS, ¹³C₈-PFOS, ¹³C₈-FOSA, d₃-MeFOSAA, d₅-EtFOSAA, ¹³C₂-4:2 FTSA, ¹³C₂-6:2 FTSA, ¹³C₂-8:2 FTSA and ¹³C₃-HFPO-DA) (Wellington

Acetic acid, ammonium acetate, and ammonium hydroxide of mass spectrometry quality and methanol of hypergrade for LC-MS quality were sourced from Sigma-Aldrich. Ultrapure water from MilliQ® IQ 7000 with an additional LC-Pack® polisher filter - a reverse-phase C18 granular silica-based cartridge was used.

2.2. Plants

Carex elata (tufted sedge) was supplied as herbal plug plants by VegTech, Sweden. These were supplied as developed tufts with a 9 cm deep, 4 cm diameter root system.

Salix Wilhelm and *Salix* Loden (willows) were supplied as cuttings by REAB, Billeberga, Sweden, and cut to 40 cm.

Cannabis sativa futura 75 (hemp) was grown from seeds in pots in Hasselfors Garden S-Soil in a greenhouse with artificial lighting for 64 days, achieving an approximate height of 100 cm before planting in the wetland.

2.3. Experimental design

The field experiments were conducted at a waste management facility in Sweden from June 14, 2022 to September 9, 2022 (87 d). In total eight wetland units each with a volume of 0.48 m³ were used (Fig. 1), including two units each planted with i) C. elata with 19 tufts each, ii) C. sativa from 18 pots (i.e. 49 and 54 stalks, respectively), iii) Salix spp with 18 S. Wilhelm and 18 S. Loden cuttings and 19 S. Wilhelm and 16 S. Loden, respectively and iv) control wetland units which were filled with the filter substrate but no plants. Water was collected from a drilled groundwater well at the facility with known PFAS contamination and pumped to a 1000 L high-density polyethylene (HDPE) buffer tank, which was level-controlled to always be filled to 700 L. The buffer tank was then used as a joint input water source to each of the 8 separate subsurface flow constructed wetland units. Each unit had a volume of 0.48 m³ (120 cm (length), 100 cm (width), 40 cm (height) and had an outer casing of HDPE covering the sides and bottom, but leaving it open upwards. The casing was filled with two permeable sections, one at each end of the wetland unit, consisting of expanded lightweight clay aggregates (LECA) (0.057 m³; 14.3 kg dw). The LECA was 12-18 mm in diameter (Saint-Gobain). In between these sections was a 0.27 m³ (62.6 kg dw) well-mixed mixture of peat, biochar, and LECA (0.1:0.1:0.8, v/ v). No additional structural elements were included to separate the

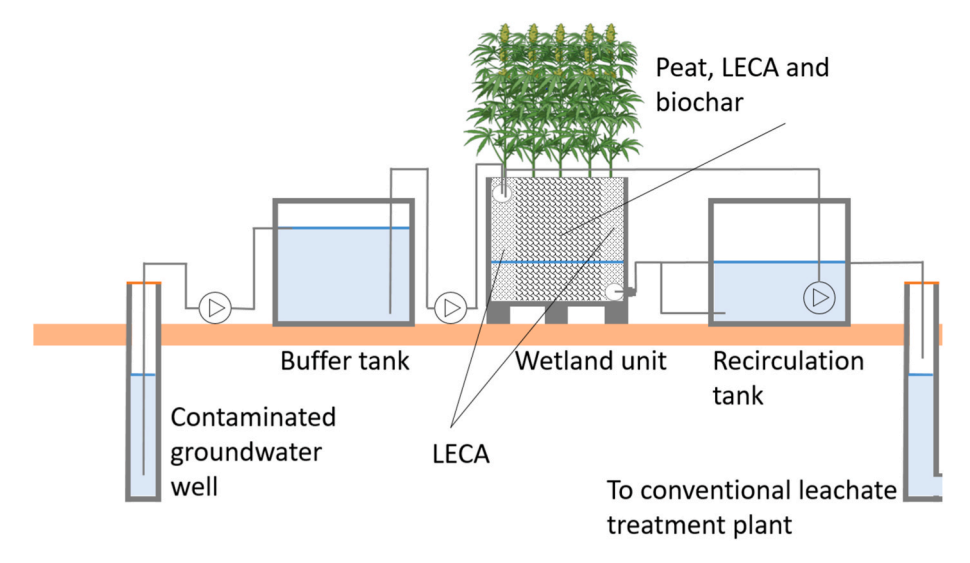


Fig. 1. Schematic of the field setup including contaminated groundwater well, buffer tank, wetland unit with substrate (peat, LECA, biochar) and i) C. elata C (C ii) C sativa C (C iii) C

permeable end sections from the central section. The substrate height in the wetland system was set at 30 cm, leaving a 10 cm HDPE headspace to allow for substrate expansion during water application. The peat was long fibered H7 from Småland, Sweden (Timfors traktor och maskin), the biochar consisted of crop production residues, pyrolyzed at 800 $^{\circ}\text{C}$ with a specific surface area (BET) of 223 m²/g, pressed into pellets with 5 mm diameter and 5-10 mm length (Skånefrö, Sweden). Water was continuously pumped from the buffer tank to the eight separate wetland units using Microdos MP2-B peristaltic pumps with a load of 50 L/d for the first 21 days, then increased to 100 L/d for the remaining 66 days of the trial. Water levels in the wetlands were set to 25 cm from the bottom for the C. elata units and 20 cm in all other cases. The pore volume of the filter substrate was estimated to be 50 %, resulting in a water volume of 150 L in the saturated zone of the C. elata and 120 L for the other units. Based on this, the hydraulic retention time in the wetland systems was estimated as follows: 72 h for C. elata with a 50 L/d load, 57.6 h for the other units with a 50 L/d load, 36 h for C. elata with a 100 L/d load, and 28.8 h for the other units with a 100 L/d load. Each wetland unit was connected to a 300 L recirculation tank to which water was transferred via an overflow mechanism. Water was continuously pumped back from the recirculation tank to its connected wetland unit at an average rate of 1090 L/d (see Table S2 in SI for the individual recirculation rates). Excess water from the recirculation tanks was discarded to a drainage system via an overflow mechanism. Water samples for PFAS were collected monthly from the overflow from the wetland units (total n =26) and the buffer tank (total n = 3) in HDPE flasks. After 87 days, plants were harvested with roots, including 3 full plants of each C. elata, S. Loden, and S. Wilhelm from both of their respective wetland units. These samples were collected diagonally across the unit to ensure spatial representation. All C. sativa were sampled from both of its wetland units (total n = 36). Composite substrate samples were collected at the end of the experiment using a Russian peat corer from the peat and biochar mixture and LECA section of the wetland in a diagonal fashion and pooled for each wetland unit (total n = 8).

2.4. Sample preparation and analysis

LECA was removed from the substrate mixture, rinsed with ultrapure MilliQ water, and analyzed separately from the peat and biochar mixture. *C. elata* plants were divided into leaf and root. *C. sativa* was divided into leaf, stem, and root. *S.* Loden and *S.* Wilhelm were divided into leaf, twig, stem, and root, where twigs were defined as the new shoots and stems as the planted cutting.

Sample preparation of peat and biochar mixture, LECA, and plant tissue was based on the method developed and validated by Nassazzi (Nassazzi et al., 2022). In the field, plant roots were rinsed with tap water to separate them from the substrate. Any remaining substrate was manually removed from the roots. All plant samples were washed with deionized water, followed by ultrapure MilliQ water, and then rinsed with 1:1 methanol and ultrapure MilliQ water. Plant, peat, and biochar mixture, and LECA samples were freeze-dried at -50 °C for 7 days and then homogenized using an IKA MultiDrive control with MultiDrive MI 250 T vessel. 0.5 g homogenized sample was spiked with $50 \mu L$ of an IS mixture ($c = 0.05 \,\mu\text{g/mL}$ for individual IS) and extracted 3 times with methanol: 1) 6 mL for 30 min, 2) 3 mL for 20 min, 3) 3 mL for 20 min in 15 mL polypropylene tubes using sonication. Each extract was transferred into a new 15 mL polypropylene tube with centrifugation at 1900g in between. Subsequently, the extract was cleaned up using ENVI carb cartridges (1 g, 12 cc, Supelco). Extracts were concentrated under N_2 to approximately 100 μL and then diluted to 500 μL with methanol.

Water samples were prepared with a method previously described (Smith et al., 2022). Briefly, 100 mL sample was filtered using a glass microfiber filter (0.7 μm , Whatman), followed by spiking with 100 μL of an IS mixture (c = 0.05 $\mu g/mL$ for individual IS) and solid phase extraction (SPE) using Oasis WAX cartridges (6 mL, 150 mg, 30 μm , Waters) eluted with 4 mL methanol followed by 4 mL 0.1 % ammonium hydroxide in methanol. Extracts were concentrated to 1 mL under nitrogen.

All samples were analyzed on an ultraperformance liquid chromatography system coupled to tandem mass spectrometry (Sciex Triple Quad 3500 UPLC-MS/MS, Phenomenex Gemini® 3 μm C18 110 Å analytical column) as previously described (Smith et al., 2022). Branched isomers of PFHpA, PFOA, PFHpS, and PFNA were quantified using their linear counterparts and should be considered semi-quantitative.

2.5. Quality control and assurance

Laboratory blanks were prepared for filter substrate (n=4), plant (n=9), and water samples (n=9). As a field blank (n=1), an HDPE sampling flask was opened during sampling and then filled with ultrapure MilliQ water that was extracted according to the protocol. As a filter blank (n=4), 100 mL ultrapure MilliQ water was filtered and extracted according to protocol. As SPE blank (n=4), a clean SPE cartridge was eluted, and the eluate was analyzed according to protocol. Method detection limits (MDL) were calculated as mean +3 times the

standard deviation (SD) of the blank samples. If a PFAS was not detected in the blanks, MDL was calculated as the mean + 3 times the SD of the lowest used calibration point. For some branched isomers (B-PFOA, B-PFHpS, B-PFNA, B-PFHpA) that did not have calibration standards, S/N = 3 for one sample of each of the matrix types was used. If the MDL was below 0.01 ng/mL, then 0.01 ng/mL, which was the lowest calibration point, was used. Three duplicate and one triplicate water sample were analyzed to assess method variability (in total, n = 9). A triplicate of plants was analyzed for one wetland unit each for C. elata, S. Loden, and S. Wilhelm to assess variability. A triplicate of each plant tissue was analyzed for C. sativa. One triplicate per plant tissue was also analyzed on a single homogenized sample to assess method variability (for details, see Tables S3-5in SI). A subset of plants from each plant species was analyzed in triplicate prior to planting in the wetland system (Tables S6.1-6.5 in SI). Samples of the peat and biochar mixture, as well as LECA, were analyzed before applying the filter substrate to the wetland units (Table S7 in SI).

2.6. Calculations and statistics

PFAS treatment efficiencies were calculated as the percentage removal of PFAS between the inlet and outlet water of each wetland unit, taken at the same time point.

Mass balances for each wetland unit were calculated, taking into account PFAS concentrations in plant biomass, filter substrate, inlet, and effluent water. Water losses through evapotranspiration have previously been estimated to 3.1 mm/d in June, 3.9 mm/d in July, 2.6 mm/d in August and 2.0 mm/d in September for a *Salix* stand in Uppsala, Sweden (Persson and Lindroth, 1994). These losses were considered negligible in relation to the flow rate of the experiment, and consequently, the effluent volume was considered equal to the inlet volume (Equation S(1) and Tables S8–11 in SI).

Total plant concentrations were calculated as the sum of the average concentration of each tissue type multiplied by the average dry weight of that tissue type, divided by the average dry weight of a whole plant. Bioconcentration factor (BCF) was calculated as PFAS concentration in plant tissue/average PFAS concentration in the inlet water (Nassazzi et al., 2023; Soda et al., 2012).

Phytoremediation potential was calculated as total plant PFAS concentration, excluding roots, multiplied by a biomass yield value derived from the literature (Zegada-Lizarazu et al., 2010; Banaszuk et al., 2020). The biomass yield value for a generic *Salix* spp used in European biomass production (Zegada-Lizarazu et al., 2010) was used as a basis for both *Salix* clones. There was a clear difference in biomass production observed between the two clones in the experiment. The literature value was thus adjusted up or down, based on the proportional difference in biomass production between the two clones, to estimate individual biomass yield values for the two clones. (For details, see equations S (2.1)-(2.4) in the SI).

The Kruskal-Wallis test with Dunn's post-hoc test was used to assess if there were any significant differences between plant tissues, roots, stems, twigs, and leaves, where applicable, regarding PFAS concentration and composition. A two-way ANOVA was performed to assess whether the distribution of PFAS with regard to concentration and composition between the plant tissue types varied significantly between the species. This analysis aimed to determine whether the species could be grouped when comparing tissue types. Subsequently, all plant species were treated as a single group to enhance statistical power when evaluating $\Sigma PFAS$ concentration, functional group distribution, and the proportion of branched compounds across tissue types.

Linear regression models were made for each species and their tissue types, with the BCF of each PFAS detected in the water phase as the response variable, the perfluoroalkyl chain length as a numerical independent variable, and functional group and isomeric configuration as categorical independent variables. All statistical analyses were carried out in R version 4.4.1.

3. Results and discussion

3.1. PFAS concentration and composition of influent and effluent water

In total, 15 out of 29 PFAS (i.e. C₄-C₉ PFCAs, C₄-C₈ PFSAs, 4:2 FTSA, 6:2 FTSA, PFECHS, and Et-FOSAA) were detected in the inlet water. With \sum PFAS concentrations of (average \pm standard error) 3870 \pm 95 ng/L (n = 3) (Fig. S1, and Tables S12.1-12.5 in SI). Both linear and branched isomers were detected for PFHpA, PFHxA, PFOA, PFHpS, PFNA, and PFOS. The same PFAS detected in the inlet could also be observed in the wetland unit outlets, with the addition of NaDONA being found above MDL in 1 sample (Control B July) and PFDA being found in two samples (Control B July and C. Sativa A July). For PFDA, this is likely due to the concentrations being close to MDL in all samples, while for NaDONA it could indicate a previous contamination in the wetland unit being washed out, or a contamination of the sample, as this peak could not be detected in any other sample throughout the experiment. NaDONA was not found in the control filter substrate analyzed prior to the experiment. However, potential contamination cannot be ruled out, as it may have originated from sources such as the HDPE casing or tubing of the wetland units.

The Σ PFAS removal efficiency (Table S13 in SI) was similar between all treatment units, including the control (15 \pm 2.5 % C. elata, 14 \pm 2.5 % *Salix* spp, 13 ± 2.5 % *C. Sativa*, 15 ± 2.6 % control) (n = 6 each). This resulted in $\Sigma PFAS$ effluent concentration of 3340 \pm 84.3 ng/L for C. sativa, 3310 \pm 89.3 ng/L for Salix spp, 3290 \pm 103 for C. elata, and 3280 ± 95.1 ng/L for the control. (Tables S12.1–12.5 in SI). The mass balance accounted for, on average, 87 \pm 0.69 % of the Σ influent PFAS. (Tables S8-11 in SI). The recovery did, however, vary across PFAS groups: short-chain PFAS and PFCAs were better accounted for (96 \pm 1.3 % and 91 \pm 0.46 % respectively) compared to long-chain PFAS, PFSAs, and precursors (82 \pm 1.4 %, 80 \pm 1.4 % and 71 \pm 2.0 % respectively). For certain individual compounds such as L-PFOS and 6:2 FTSA, the mass balance recovery was notably lower (40 \pm 1.3 % and 35 \pm 4.2 % respectively). The low mass balance recovery of PFAS precursors may be partially attributed to their transformation within the plants and the wetland system, as reported previously (Fang et al., 2024; Zhao et al., 2019). In contrast, the low recovery of long-chain PFAS and PFSAs, like PFOS, is more likely due to sorption onto suspended particles, subsequently removed during filtration before analysis, which has been previously reported (Sörengård et al., 2020). The wetland systems may have contributed additional suspended particles, thereby influencing the mass balance recovery. Substantial algae growth was observed in the recirculation tanks, which may also have contributed to an increase in suspended particles in the effluent water samples. Additional factors potentially contributing to the incomplete mass balance for the long-chain PFAS include sorption to pipes and outer walls of the setup, as well as to the sampling flasks. Furthermore, sorption to the external surfaces of plant roots may also have influenced the mass balance, as this PFAS fraction was not analyzed. Therefore, the reported removal efficiencies for certain PFAS are likely overestimated. The similarity in treatment efficiency between the planted wetland units and the controls indicates that the main PFAS removal mechanism of the wetland units was the filter substrate. This theory is further supported by the treatment efficiencies for the individual PFAS, where long-chain PFAS and PFSAs were more efficiently removed than short-chain PFAS and PFCAs, even when accounting for their lower mass balance recoveries. Hereby, L-PFOS had the highest removal efficiencies with 80-63 %, and PFBA had the lowest removal efficiencies with -3.2 to 8.5%, excepting B-PFNA, which showed highly variable removal efficiencies with -25 to 26 %. This could be attributed to the previously reported higher sorption capacity of longer chain PFAAs to soil matrices compared to shorter chain PFAAs (Li et al., 2019b). The high variability in PFNA removal is likely due to concentrations being close to the MDL. The fact that the addition of plants did not give any additional decrease in PFAS concentration in the treated water could be attributed to the

high water flow used in the experiment (on average, 87.9 L/d).

The difference in treatment efficiency for different branched and linear PFAS led to changes in the isomeric composition of several compounds, where the branched isomer fraction increased after treatment. This trend was observed in both the planted wetland units and the controls, with the most notable example being PFOS, where branched PFOS-isomers increased from 40 % to 62 % of Σ PFOS. This could also be seen in PFNA (27 %-36 %) and PFHpS (33 %-39 %). This could be expected as branched isomers such as PFOA and PFOS have been reported to be enriched in solution compared to sediment in river water, due to their lower hydrophobicity compared to their linear counterparts (Chen et al., 2015). Change in isomeric composition was not observed for PFHpA, PFHxS, or PFOA, possibly due to the difference in combined linear and branched isomer treatment efficiency of the wetland units for the different PFAS. The average removal efficiencies for ΣPFHpS, PFOS, and PFNA across all wetland units, including the controls, were 29 %, 33 %, and 57 %, respectively. Meanwhile, the treatment efficiencies for ΣPFHxS, PFHpA, and PFOA were lower, at 16 %, 11 %, and 19 %, respectively.

3.2. PFAS uptake and concentrations in the plants and filter substrate

In total, 19 out of 29 PFAS (i.e., C3-C11 PFCAs, C4-C8 PFSAs, PFECHS, FOSA, 6:2 FTSA, 8:2 FTSA, and Et-FOSAA) (n = 8) were detected in the peat and biochar, excluding the LECA (Fig. 2, Tables S14.1-14.5 in SI). This includes four PFAS (PFDA, PFDoDA, FOSA, and 8:2 FTSA), which were not detected in the influent water. PFDA and PFDoDA were also found in low concentrations in the control substrate, suggesting that these compounds may have been present in the filter substrate prior to the experiment. As for the presence of FOSA and 8:2 FTSA, this could be attributed either to contamination from other components of the wetland units, such as the HDPE surfaces or tubing, or to accumulation and subsequent up-concentration to detectable levels during the experimental period. These compounds have relatively long perfluoroalkyl chains, which are correlated to a high solid-water partitioning coefficient in carbon-rich materials such as biochar (Fabregat-Palau et al., 2022), thus supporting the up-concentration theory. The fluorotelomer 4:2 FTSA, while present in the influent water, was not detected in the peat and biochar. Fluorotelomers are

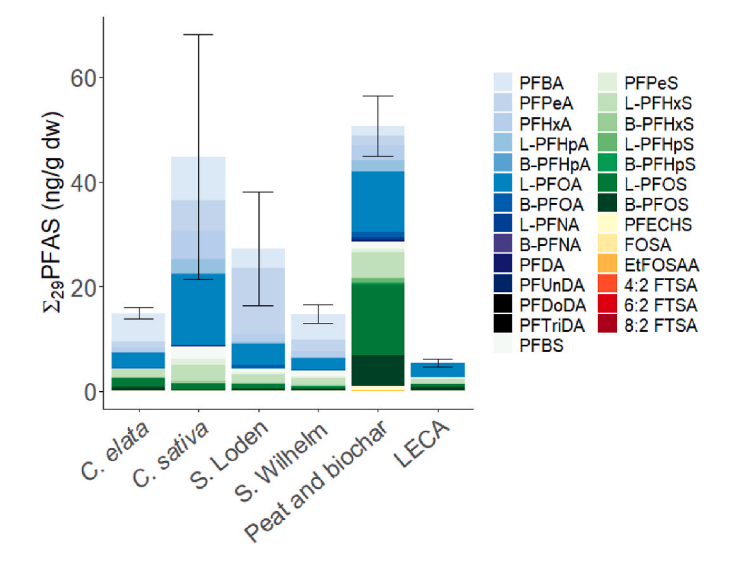


Fig. 2. Total plant ΣPFAS concentration in the different plant species (each n=2) (including roots, twigs, stem, leaves), peat and biochar mixture (n=8), and LECA (n=8). PFCAs are represented in blue, PFSAs in green, and other functional groups in yellow and red. Error bars represent the standard error. (For interpretation of the references to colour in this figure legend, the reader is referred to the Web version of this article.)

known to be transformed to PFAAs in river sediment (Zhang et al., 2016a), which is likely to also occur in the wetland units. Both linear and branched isomers were detected for PFNA, PFHxS, PFHpS, and PFOS. The variations in Σ PFAS concentration of the peat and biochar, comparing the different wetland units, including the controls, were low, with average Σ PFAS being 56.2 \pm 9.65 ng/g dw (*C. elata*), 54.1 \pm 16.5 ng/g dw (control), 48.1 \pm 9.27 ng/g dw (*C. sativa*), and 44.4 \pm 19.8 ng/g dw (*Salix* spp), (n=2 each).

Only eight out of 29 PFAS (Fig. 2, Tables S14.1-14.5 in SI) (n = 8) (i. e., PFOA, PFTriDA, C₄-C₈ PFSAs, and PFECHS) were detected in LECA, ranging from 3.38 ng/g dw (*Salix* spp) to 7.92 ng/g dw (control) for \sum PFAS (n = 2 each).

In total, 15 out of 29 PFAS were detected in the plants (n = 8)(including roots, twigs, stems, and leaves). 12 out of 29 PFAS were detected in all plant species (i.e. C3-C7 PFCAs, C4-C8 PFSAs, PFECHS, and FOSA) (Fig. 2, Tables S15.1-15.5 in SI). Both linear and branched isomers were detected for PFHxS, PFOA, PFHpS, PFNA, PFOS, and PFHpA. Uptake of PFNA was only found in C. elata and C. sativa, and uptake of PFDA and PFUnDA was only found in C. sativa. The fluorotelomeres 4:2 FTSA and 6:2 FTSA, while present in the inlet water, were not found in any plant. These compounds have been shown to be enzymatically transformed to PFAAs by plants (Zhao et al., 2019; Zhang et al., 2016b; Zhao et al., 2018), which may explain why they were not detected in the plants. Et-FOSAA is another PFAS found in the inlet water, which is known to transform in nature (Mejia Avendaño and Liu, 2015), and was not found in any plant. PFDA and PFUnDA were detected in C. sativa, but not in the influent water. This could be explained by the accumulation and up-concentration of these compounds to detectable levels in the plant tissue. PFDA was also found in the peat and biochar, making it possible that C. sativa took up PFDA from the filter substrate. Total plant \sum PFAS concentrations were highest in *C. sativa* (44.7 \pm 23.4 ng/g dw), followed by S. Loden (19.4 \pm 10.9 ng/g dw), C. elata (14.9 \pm 1.07 ng/g dw), and S. Wilhelm (14.7 \pm 1.72 ng/g dw) (n=2 each). It should be noted, though, that some of the PFAS detected in plant tissue may derive from foliar uptake rather than from the inlet water, as foliar uptake of PFAS has previously been shown to occur (Chen et al., 2024).

Consequently, our results show that PFAS accumulate in both plant tissue and substrate, which is consistent with the findings of previous studies (Sharma et al., 2020; Dalahmeh et al., 2019; Campos-Pereira et al., 2022). However, to the best of our knowledge, the capture of PFAS in a combined peat and biochar mixture subsurface flow wetland with growing plants has not been reported previously.

The composition of PFAS differed between the sample matrix types (Fig. 2, Tables S14.1-S14.5, and S15.1-15.5 in SI). In the total plants (including roots, leaves, twigs, and stems where applicable), PFCAs had the highest contribution (77 % of ∑PFAS), followed by PFSAs (23 %) and \(\sum \) precursors (0.69 %). The PFAS composition in plants was dominated by short-chain C_3 - C_6 PFCAs and C_4 - C_5 PFSAs (57 % of Σ PFAS), whereas the peat and biochar mixture and LECA had a high contribution of long-chained C7-C12 PFCAs and C6-C8 PFSAs (77 % and 93 % of \sum PFAS, respectively). The peat and biochar mixture and the LECA had a higher fraction of PFSAs (54 % and 51 % of ∑PFAS, respectively) compared to the water and plant samples (26 % and 23 % of ∑PFAS, respectively). This difference in composition could be attributed to the higher sorption capacity of longer chain PFAAs as well as PFSAs to soil matrices (Li et al., 2019b). The shorter chain PFAS with a lower sorption capacity instead becomes available for plant uptake, which has also been observed in earlier studies (Nassazzi et al., 2023; Zhang et al., 2020). The distribution of the PFAS precursors also varied, with the peat and biochar mixture and LECA having a slightly higher fraction (1.9 % and 2.3 % of \(\sumeter PFAS,\) respectively) compared to the water (1.4 % of \(\sum_{PFAS} \), and the plant samples having a lower fraction (0.69 \% of Σ PFAS). The low contribution of PFAS precursors in plants could be due to the enzyme-mediated transformation of PFAS precursors to perfluorinated compounds, which are known to take place within several PFAS precursor groups (Zhao et al., 2019; Zhang et al., 2016b; Zhao

et al., 2018).

3.3. Tissue distribution of PFAS in the plant roots, stems, twigs, and leaves

The two-way ANOVA model revealed no significant differences in composition between tissue types across species in terms of \sum PFAS concentration, fraction of functional groups, and fraction of branched isomers (p > 0.05). All species were thus pooled in the statistical analysis for these measurements to increase statistical power.

The \(\sumset \text{PFAS} \) concentration varied between different plant tissue types (Fig. 3). The PFAS concentrations were significantly higher in the leaves (Σ PFAS = 111 \pm 38.7 ng/g dw) compared to the roots (Σ PFAS $= 10.9 \pm 1.73 \text{ ng/g dw}$), $> \text{stems} (\sum PFAS = 4.79 \pm 2.28 \text{ ng/g dw}) >$ and twigs (\sum PFAS = 2.26 \pm 1.29 ng/g dw) for all plant species (p <0.05). Note that the twig tissue was only present in S. Wilhelm and S. Loden. Furthermore, ∑PFAS concentrations in roots were significantly higher compared to twigs (p < 0.05). Comparing the functional groups of PFAS, in roots, PFSAs were the largest PFAS fraction (on average, 66 % of Σ PFAS) compared to PFCAs (32 %), and Σ precursors (2.1 %). Contrastingly, in leaves, the PFCAs comprised the highest composition (on average, 84 % of ∑PFAS) compared to PFSAs (16 %) and ∑precursors (0.35 %). In stem and twigs, the PFAS composition profile was more evenly distributed between PFSAs (on average, 41 % and 57 % of Σ PFAS, respectively) and PFCAs (53 % and 46 %, respectively), but low for ∑precursors (1.8 % and 0.95 %, respectively). The different distribution of PFAS regarding concentration and functional group has been previously reported (Nassazzi et al., 2023), and indicates a correlation of these factors with the translocation of PFAS from roots to leaves.

3.4. Bioconcentration factors (BCF)

The BCF for individual PFAS ranged from 0.24 to 179 for leaves, stems, twigs, and roots (Fig. 4). The highest BCF value for *C. sativa*, S. Wilhelm, and *C. elata* was that of PFBA (137, 129, and 42.7,

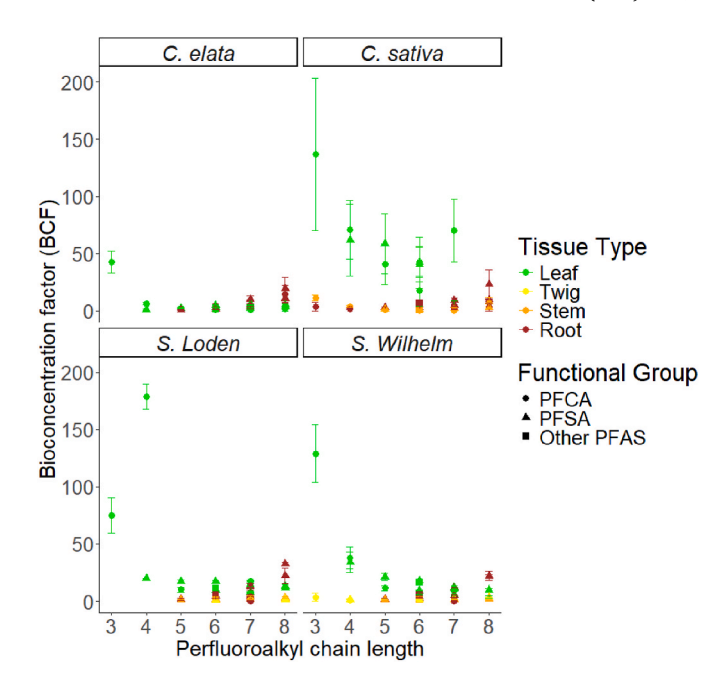


Fig. 4. PFAS bioconcentration factors (BCF = $C_{plant\text{-}tissue}/C_{Inlet\text{-}water}$) in different plant tissues plotted against the perfluoroalkyl chain length of the PFAS, n=2 per species.

respectively) in leaves, which is comparable to what has previously been observed for sunflower, mustard, *Salix eleagnos*, and *Salix purpurea* (Nassazzi et al., 2023; Sharma et al., 2020). The highest BCF for S. Loden, however, was found for PFPeA (179) in leaf. All detected < C7 PFAS had a higher BCF in leaf tissue than in root tissue in all plants, whereas all detected > C8 PFAS had a higher BCF in root tissue than in leaf tissue in all plants. These results are further strengthened by the linear regression model showing a significant positive correlation (p <

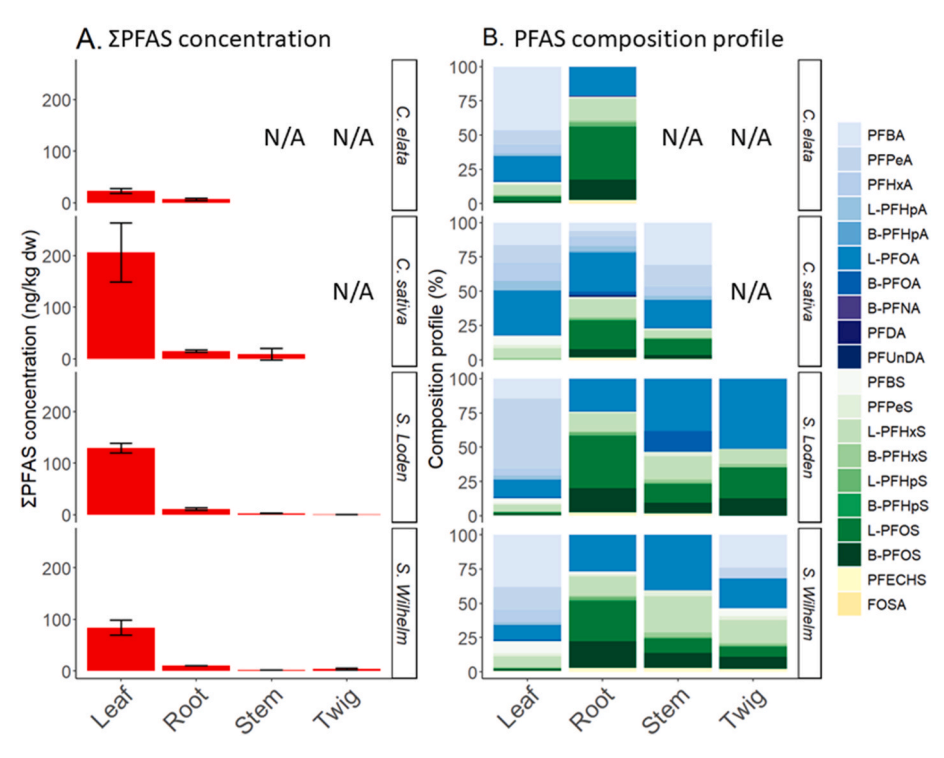


Fig. 3. A) Σ PFAS concentration in different plant tissue types (n=2), and B) PFAS composition profile of each tissue type. *C. sativa* did not have twigs, and *C. elata* did not have twigs or stems; thus, these tissue types are not applicable (N/A). PFCAs are represented in blue, PFSAs in green, and other functional groups in yellow. (For interpretation of the references to colour in this figure legend, the reader is referred to the Web version of this article.)

0.05) between the perfluoroalkyl chain length and BCF in the root tissue for all species except C. sativa, for which it was seen but not significant (p = 0.07). Inversely, there was a significant negative correlation between BCF and perfluoroalkyl chain lengths for the leaf tissue in C. sativa and S. Wilhelm (p < 0.05), which was also seen but not significant for the other species (p = 0.063-0.096). The BCF in stems and twigs was lower than that of either leaves or roots for every detected PFAS. This can be expected as PFAS with a high sorption coefficient to plant tissue will be immobilized and accumulated in the roots, while PFAS with a low sorption coefficient to plant tissue will be transported to the leaf without sorption to stem or twigs, as reported previously (Felizeter et al., 2014; Battisti et al., 2023). The linear regression model showed no significant correlation between chain length and BCF in twigs or stems (p > 0.05). Regarding the impact of the PFAS functional group, the linear regression models indicated that the sulfonic group had a positive impact on BCF in stems and roots of the two Salix clones compared to the carboxylic group. This was, however, only significant for S. Wilhelm (p < 0.05). If instead directly comparing the BCF for PFCAs and PFSAs with the same perfluoroalkyl chain length, there was a higher BCF for C5-C8 PFSAs compared to C5-C8 PFCAs in all species, for root, stem, and twig tissue, with the exception of C₇ PFCA (PFOA) having a higher BCF than its corresponding PFSA in S. Loden stem, and some PFSAs being below MDL in S. Loden twigs. This is expected since PFSAs have been shown to have a higher sorption capacity to the root tissue than PFCAs (Felizeter et al., 2014), which would allow for increased accumulation in roots but reduced transport to leaves. Supporting this theory, the BCF for C₄ PFCA (PFPeA) was higher than that of C4 PFSA (PFBS) for all species in leaf tissue. However, the BCF of C5-C8 PFSAs was higher than that of their corresponding PFCAs for all species in leaf tissue, except for C7-C8 PFAS in C. sativa. This could perhaps be explained by the large differences in the inlet water concentration of these compounds (Fig. S1 in SI). The difference in BCF between tissue types has been observed previously (Nassazzi et al., 2023; Sharma et al., 2020; Battisti et al., 2023) and is most likely due to the negative correlation between PFAS hydrophobicity and their mobility from roots to above-ground plant parts. It has been proposed that the casparian strip, a selective barrier in the plant root, plays a major role in the translocation of PFAS within the plant (Felizeter et al., 2014; Felizeter et al., 2012). Less hydrophobic, shorter-chain PFAS may be able to cross the casparian strip into the plant vascular tissue and be further translocated to above-ground plant parts through the xylem. More hydrophobic, longer-chained PFAS are restricted and tend to accumulate in the outer root tissues. This was supported by a study on fern roots, which found PFOS in the root cortex (outside the casparian strip), whereas the less hydrophobic GenX was only found near the vascular cylinder (inside the casparian strip) (Qian et al., 2023). This could also reflect PFOS sorption to the tissues of the root cortex. Additional evidence from a comparative study with radish and pak choi indicated that the absence of a functional Casparian strip in radish allowed for greater translocation of PFOA in the radish compared to the pak choi (Xu et al., 2024).

3.5. Estimated treatment potential using phytoremediation

All species had above-ground tissue/water concentrations >10/1 for PFBA. This was also the case for C. elata with L-PFOS, and C. sativa with PFPeA, PFBS, PFPeS, and L-PFOA, and S. Loden with PFPeA. The phytoremediation potential for PFAS for the four investigated plant species was estimated based on the PFAS concentration in the plant (i.e., sum of the total mass in stem, twigs, and leaves) and biomass production per ha and year (Table 1). C. sativa had the highest predicted removal capacity for Σ PFAS (941 \pm 670 mg Σ PFAS/ha yr) due to both the highest PFAS concentration in this study and the high biomass yields reported in the literature (Zegada-Lizarazu et al., 2010). C. elata had the lowest predicted removal capacity for Σ PFAS (164 \pm 56 mg Σ PFAS/ha yr), partly because of its lower reported biomass yields (Banaszuk et al., 2020). The results correspond well with a previous study estimating the phytoremediation removal potential of Norway spruce, silver birch, and ground elder close to a PFAS-impacted airfield to 550-1400 mg/ha yr of Σ_{26} PFAS (Gobelius et al., 2017). It is, however, important to note that the total removal of PFAS by phytoremediation is dependent on PFAS concentration, as an increase in PFAS concentration has been shown to lead to an increase in PFAS uptake in plants (Gredelj et al., 2020). Cultivation methods have also been proven to be important, as is shown by the difference in BCF for different PFAS between hydroponic and soil conditions (Gredelj et al., 2020). It is reasonable to also extend this to include different soil types, especially since factors like pH have been shown to play a role in plant uptake of PFAS (Krippner et al., 2014). It is also likely that the removal values in Table 1 are underestimated, as the hydraulic retention time in the wetland units was likely too low to achieve effective treatment. Previous studies have used both considerably higher and lower retention times than those used in this study (Ferrario et al., 2022; Soda et al., 2012). A higher retention time would likely increase the fraction of the water removed through transpiration, which would likely also increase the relative PFAS uptake and immobilization in plant tissues. It would also result in a higher fraction of the water being lost to evaporation, thus increasing the PFAS concentration in the remaining water, which has been shown to increase plant uptake of PFAS (Gredelj et al., 2020). This could, however, also prove problematic for leachate-impacted groundwater with high sodium chloride concentrations, as the salt would accumulate in the wetland, which might prove detrimental to the plants. Both Salix and C. sativa are reported to be cultivated on industrial scales for bioenergy purposes due to their high biomass yields (Zegada-Lizarazu et al., 2010), suggesting that they would be suitable for phytoremediation of PFAS. However, it has been reported that adding nutrients to stimulate biomass growth reduces the PFAS concentrations in plant tissue (Nassazzi et al., 2023), showing that the subject of phytoremediation is more complicated than the maximization of biomass, since if this were the case, PFAS concentration in plant tissue would have remained constant for plants receiving nutrients, thus increasing the total PFAS uptake. C. elata is typically not cultivated for biomass purposes and has considerably lower biomass yields than C. sativa and Salix (Banaszuk et al., 2020; Zegada-Lizarazu, 2010). On the other hand, the Carex genus has been considered in previous PFAS phytoremediation studies (Greger, 2021; Zhang et al.,

Table 1
Estimated treatment potential for the different plant species derived from \sum PFAS concentrations (for individual PFAS see Tables S16–S20 in SI) derived in this study, combined with literature values on expected biomass yields (stem, twigs, leaves). A median value is calculated based on the biomass range. The biomass values of both Salix spp and C. sativa were obtained from the same publication.

Species	Mean Σ PFAS concentration (ng/g dw) (range)	Tonnes of biomass (stem, twigs, leaves) range in dw/ha yr	Median Σ PFAS removed in mg dw/ha yr (range)
C. elata	$22.8 \pm 4.73 \ (18.1 – 27.5)$	6-8(Banaszuk et al., 2020)	164 ± 56 (108–220)
C. sativa	$48 \pm 25 \ (22.6 – 73.4)$	12-22 (Zegada-Lizarazu et al., 2010)	$941 \pm 670 \ (271 – 1610)$
S. Wilhelm	$14.7 \pm 1.7 \ (13.1 – 16.6)$	13–30 ^a (Zegada-Lizarazu et al., 2010)	$333 \pm 163 (170 496)$
S. Loden	$19.5 \pm 11 \ (8.5 – 30.5)$	10-23 ^a (Zegada-Lizarazu et al., 2010)	$393 \pm 308 \ (85-702)$

^a Biomass yields for the different *Salix* clones were taken from the mean *Salix* production data (Zegada-Lizarazu et al., 2010) and adjusted for biomass differences seen in the experiment.

2021a). In this study, however, *C. elata* showed lower phytoremediation potential compared to *C. sativa* or *Salix*.

The modest PFAS removal shown by plants in wetland systems in this study suggests that this approach is best suited for smaller-scale, local water treatment applications where conventional PFAS treatment options may be cost-prohibitive. Such scenarios include agricultural runoff, stormwater, leachate from small waste management facilities, gray water, or decentralized sewage treatment systems. These wetlands are particularly beneficial for treating complex waters co-contaminated with metals or nutrients, as constructed wetlands have been shown to efficiently remove these contaminants (Sheoran and Sheoran, 2006; Vymazal, 2007). If safe end-use of the harvested biomass can be ensured, such as through hydrothermal liquefaction to produce bio-oil and biochar (Zhang et al., 2021b), it could also offer value recovery from PFAS-contaminated land, irrigation water, or fertilizers, while at the same time contributing to system remediation.

4. Conclusions

This study investigated the use of subsurface flow constructed wetlands, with plants, to treat landfill leachate-impacted groundwater during field conditions. The main removal mechanism of the wetlands was shown to be sorption by the peat and biochar filter substrate, due to short residence times in the units. Although plant uptake and accumulation of PFAS were also observed. Short-chain PFAS and PFCAs were shown to be taken up and translocated to above-ground plant parts, while long-chain PFAS and PFSAs accumulated in plant roots and the filter substrate. The above-ground BCF was >10 for several PFAS in one or more plant species (PFBA, PFPeA, L-PFOA, PFBS, PFPeS, and L-PFOS), with *C. Sativa* having an above-ground BCF >10 for the highest amount of different PFAS. The study shows how plants can be used in combination with a peat and biochar filter substrate to treat PFAScontaminated groundwater, removing both short and long-chain PFAS. The study thus provides valuable insight into how full-scale wetland systems could be designed for efficient PFAS treatment. It is, however, important to acknowledge the limitations of operating pilot wetlands for a single growing season. Further studies should focus on larger-scale systems operated for several seasons. It is also important to look into the regeneration or destruction of the filter substrate, as well as the safe repurposing or destruction of harvested biomass. It is also important to design the wetland and its recirculation to limit the creation of aerosols and PFAS transport to the atmosphere. The removal efficiencies of plants observed in this study suggest that phytoremediation of PFAS contaminated water using wetlands would be best suited for smaller-scale, local systems such as the treatment of agricultural runoff, stormwater, leachate from small waste management facilities, greywater, or decentralized sewage treatment systems. To achieve effective treatment, hydraulic retention times in such systems would likely need to be longer than those applied in this study. Other uses for this technology is where safe use of harvested biomass, such as for biofuel or biochar production, can enable the beneficial use of PFAS-contaminated irrigation water or fertilization. Our study has shown that phytoextraction of PFAS was most efficient for the removal of short-chain PFAS, suggesting that it could be a viable method in combination with other methods proven to be efficient for the removal of long-chain PFAS, such as activated carbon filters or foam fractionation.

CRediT authorship contribution statement

Oscar Liljeström: Writing – original draft, Software, Methodology, Investigation, Formal analysis, Data curation, Conceptualization. Dahn Rosenquist: Writing – review & editing, Methodology, Funding acquisition, Conceptualization. Dan B. Kleja: Writing – review & editing, Supervision, Funding acquisition. Anja Enell: Writing – review & editing, Supervision, Funding acquisition. Lutz Ahrens: Writing – review & editing, Supervision, Methodology, Funding acquisition,

Conceptualization.

Declaration of competing interest

The authors declare the following financial interests/personal relationships which may be considered as potential competing interests: Oscar Liljestrom reports equipment, drugs, or supplies was provided by Laqua Treatment AB. Dahn Rosenqvist reports a relationship with Laqua Treatment AB that includes: employment. If there are other authors, they declare that they have no known competing financial interests or personal relationships that could have appeared to influence the work reported in this paper.

Acknowledgements

This work was part of the LIFE SOURCE project (LIFE20 ENV/ES/ 000880), which has received funding from the LIFE program of the European Union. We also wish to acknowledge the staff at the waste management facility who have been very supportive during the project.

Appendix A. Supplementary data

Supplementary data to this article can be found online at https://doi.org/10.1016/j.envpol.2025.127199.

Data availability

Data will be made available on request.

References

- Ali, H., Khan, E., Sajad, M.A., 2013. Phytoremediation of heavy metals-Concepts and applications. Chemosphere 91, 869–881.
- Askeland, M., et al., 2020. Biochar sorption of PFOS, PFOA, PFHxS and PFHxA in two soils with contrasting texture. Chemosphere 249, 126072.
- Awad, J., et al., 2022. Application of native plants in constructed floating wetlands as a passive remediation approach for PFAS-impacted surface water. J. Hazard. Mater. 429, 128326.
- Banaszuk, P., Kamocki, A.K., Wysocka-Czubaszek, A., Czubaszek, R., Roj-Rojewski, S., 2020. Closing the loop - recovery of nutrients and energy from wetland biomass. Ecol. Eng. 143, 105643.
- Barry, V., Winquist, A., Steenland, K., 2013. Perfluorooctanoic acid (PFOA) exposures and incident cancers among adults living near a chemical plant. Environ. Health Perspect. 121, 1313–1318.
- Battisti, İ., et al., 2023. Perfluoroalkyl substances exposure alters stomatal opening and xylem hydraulics in willow plants. Chemosphere 344, 140380.
- Beale, D.J., et al., 2022. Host-gut microbiome metabolic interactions in PFAS-impacted freshwater turtles (Emydura macquarii macquarii). Metabolites 12, 1–19.
- Birnstingl, J., Wilson, J., 2024. A cost comparison of pump-and-treat and in situ colloidal activated carbon for PFAS plume management. Remed. J. 35.
- Brunn, H., et al., 2023. PFAS: forever chemicals—persistent, bioaccumulative and mobile. Reviewing the status and the need for their phase out and remediation of contaminated sites. Environ. Sci. Eur. 35, 1–50.
- Brusseau, M.L., 2024. Field versus laboratory measurements of PFAS sorption by soils and sediments. J. Hazard. Mater. Adv. 16, 100508.
- Campos-Pereira, H., et al., 2022. Binding of per- and polyfluoroalkyl substances (PFASs) by organic soil materials with different structural composition charge- and concentration-dependent sorption behavior. Chemosphere 297.
- Chen, X., et al., 2015. Isomeric specific partitioning behaviors of perfluoroalkyl substances in water dissolved phase, suspended particulate matters and sediments in Liao River Basin and Taihu Lake, China. Water Res. 80, 235–244.
- Chen, X., et al., 2024. Multimedia and full-life-cycle monitoring discloses the dynamic accumulation rules of PFAS and underestimated foliar uptake in wheat near a fluorochemical industrial Park. Environ. Sci. Technol. https://doi.org/10.1021/acs. est.4c03525.
- Dalahmeh, S.S., Alziq, N., Ahrens, L., 2019. Potential of biochar fi Iters for onsite wastewater treatment: effects of active and inactive bio fi Ims on adsorption of perand poly fl uoroalkyl substances in laboratory column experiments. Environ. Pollut. 247, 155–164.
- Fabregat-Palau, J., Vidal, M., Rigol, A., 2022. Examining sorption of perfluoroalkyl substances (PFAS) in biochars and other carbon-rich materials. Chemosphere 302, 134733.
- Fang, B., et al., 2024. Fluorotelomer betaines and sulfonic acid in aerobic wetland soil: stability, biotransformation, and bacterial community response. J. Hazard. Mater. 477, 135261.

- Felizeter, S., McLachlan, M.S., De Voogt, P., 2012. Uptake of perfluorinated alkyl acids by hydroponically grown lettuce (Lactuca sativa). Environ. Sci. Technol. 46, 11735–11743.
- Felizeter, S., Mclachlan, M.S., Voogt, P. De, 2014. Root Uptake and Translocation of per Fl Uorinated Alkyl Acids by Three Hydroponically Grown Crops.
- Fenton, S.E., et al., 2021. Per- and polyfluoroalkyl substance toxicity and human health review: current state of knowledge and strategies for informing future research. Environ. Toxicol. Chem. 40, 606–630.
- Ferrario, C., et al., 2022. Assessment of reed grasses (Phragmites australis) performance in PFAS removal from water: a phytoremediation pilot plant study. Water (Switzerland) 14.
- Gaines, 2022. Historical and Current Usage of Per- and Polyfluoroalkyl Substances PFAS A.Pdf.
- Gan, S., Lau, E.V., Ng, H.K., 2009. Remediation of soils contaminated with polycyclic aromatic hydrocarbons (PAHs). J. Hazard. Mater. 172, 532–549.
- Gobelius, L., Lewis, J., Ahrens, L., 2017. Plant uptake of Per- and polyfluoroalkyl substances at a contaminated fire training facility to evaluate the phytoremediation potential of various plant species. Environ. Sci. Technol. 51, 12602–12610.
- Gredelj, A., et al., 2020. Uptake and translocation of perfluoroalkyl acids (PFAAs) in hydroponically grown red chicory (Cichorium intybus L.): growth and developmental toxicity, comparison with growth in soil and bioavailability implications. Sci. Total Environ. 720, 137333.
- Greger, M., 2021. Removal of PFAS from water by plants. Int. J. Environ. Sci. Nat. Resour. 28, 1–6.
- Hale, S.E., et al., 2017. Sorbent amendment as a remediation strategy to reduce PFAS mobility and leaching in a contaminated sandy soil from a Norwegian firefighting training facility. Chemosphere 171, 9–18.
- Hepburn, E., et al., 2019. Contamination of groundwater with per- and polyfluoroalkyl substances (PFAS) from legacy landfills in an urban re-development precinct. Environ. Pollut. 248, 101–113.
- Huff, D.K., Morris, L.A., Sutter, L., Costanza, J., Pennell, K.D., 2020. Accumulation of six PFAS compounds by woody and herbaceous plants: potential for phytoextraction. Int. J. Phytoremediation 22, 1538–1550.
- Kang, Y., Guo, Z., Ma, H., Wu, H., Zhang, J., 2023. Enhanced removal of perfluorooctanoic acid (PFOA) and perfluorooctane sulfonate (PFOS) in constructed wetlands: iron cycling and microbial mechanisms. ACS ES T Water 3, 287–297.
- Kasak, K., et al., 2018. Biochar enhances plant growth and nutrient removal in horizontal subsurface flow constructed wetlands. Sci. Total Environ. 639, 67–74.
- Kelly, B.C., et al., 2009. Perfluoroalkyl contaminants in an arctic marine food web: Trophic magnification and wildlife exposure. Environ. Sci. Technol. 43, 4037–4043. Perfluoroalkyl.
- Krippner, J., et al., 2014. Effects of chain length and pH on the uptake and distribution of perfluoroalkyl substances in maize (Zea mays). Chemosphere 94, 85–90.
- Kwok, K.Y., et al., 2015. Occurrence and distribution of conventional and new classes of per- and polyfluoroalkyl substances (PFASs) in the South China Sea. J. Hazard. Mater. 285, 389–397.
- Laramay, F., Crimi, M., 2020. Theoretical evaluation of chemical and physical feasibility of an in situ ultrasonic reactor for remediation of groundwater contaminated with per- and polyfluoroalkyl substances. Remediation 31, 45–58.
- Lesmeister, L., et al., 2021. Extending the knowledge about PFAS bioaccumulation factors for agricultural plants a review. Sci. Total Environ. 766, 142640.
- Li, J., Fan, J., Liu, D., Hu, Z., Zhang, J., 2019a. Enhanced nitrogen removal in biocharadded surface flow constructed wetlands: dealing with seasonal variation in the north China. Environ. Sci. Pollut. Res. 26, 3675–3684.
- Li, F., et al., 2019b. Adsorption of perfluorinated acids onto soils: Kinetics, isotherms, and influences of soil properties. Sci. Total Environ. 649, 504–514.
- Lott, D.J., Robey, N.M., Fonseca, R., Bowden, J.A., Townsend, T.G., 2023. Behavior of Per- and polyfluoroalkyl substances (PFAS) in pilot-scale vertical flow constructed wetlands treating landfill leachate. Waste Manag. 161, 187–192.
- Ma, H., et al., 2023. Enhancement of perfluorooctanoic acid and perfluorooctane sulphonic acid removal in constructed wetland using iron mineral: performance and mechanisms. J. Hazard. Mater. 447, 130819.
- Mejia Avendaño, S., Liu, J., 2015. Production of PFOS from aerobic soil biotransformation of two perfluoroalkyl sulfonamide derivatives. Chemosphere 119, 1084–1090.
- Nason, S.L., et al., 2024. A comprehensive trial on PFAS remediation: hemp phytoextraction and PFAS degradation in harvested plants. Environ. Sci. Adv. 3, 304–313
- Nassazzi, W., Lai, F.Y., Ahrens, L., 2022. A novel method for extraction, clean-up and analysis of per- and polyfluoroalkyl substances (PFAS) in different plant matrices using LC-MS/MS. J. Chromatogr., B: Anal. Technol. Biomed. Life Sci. 1212, 123514.
- Nassazzi, W., Wu, T.C., Jass, J., Lai, F.Y., Ahrens, L., 2023. Phytoextraction of per- and polyfluoroalkyl substances (PFAS) and the influence of supplements on the performance of short-rotation crops. Environ. Pollut. 333, 122038.
- Nelson, J.W., Hatch, E.E., Webster, T.F., 2010. Exposure to polyfluoroalkyl chemicals and cholesterol, body weight, and insulin resistance in the general U.S. population. Environ. Health Perspect. 118, 197–202.

- OECD, 2021. Reconciling terminology of the universe of Per- and polyfluoroalkyl substances: recommendations and practical guidance. OECD Ser. Risk Manag. 61, 1–45.
- Persson, G., Lindroth, A., 1994. Hydrology simulating evaporation from short-rotation forest: variations within and between seasons. J. Hydrol. 156.
- Philip, McCleaf, Sophie, Englund, Anna, Östlund, Lindegren, Klara, Wiberg, Karin, Lutz, Ahrens, 2017. Removal efficiency of multiple poly- and perfluoroalkyl substances (PFASs) in drinking water using granular activated carbon (GAC) and anion exchange (AE) column tests. Water Res. 120, 77–87.
- Qian, S., et al., 2023. Bioaccumulation of Per- and polyfluoroalkyl substances (PFAS) in ferns: effect of PFAS molecular structure and plant root characteristics. Environ. Sci. Technol. 57, 4443–4453.
- Rauert, C., Shoieb, M., Schuster, J.K., Eng, A., Harner, T., 2018. Atmospheric concentrations and trends of poly- and perfluoroalkyl substances (PFAS) and volatile methyl siloxanes (VMS) over 7 years of sampling in the global Atmospheric Passive Sampling (GAPS) network. Environ. Pollut. 238, 94–102.
- Salt, D.E., Smith, R.D., Raskin, I., 1998. Phytoremediation. Annu. Rev. Plant Biol. 49, 643–668.
- Sharma, N., et al., 2020. Accumulation and effects of perfluoroalkyl substances in three hydroponically grown Salix L. species. Ecotoxicol. Environ. Saf. 191.
- Sheoran, A.S., Sheoran, V., 2006. Heavy metal removal mechanism of acid mine drainage in wetlands: a critical review. Miner. Eng. 19, 105–116.
- Smith, S.J., Wiberg, K., McCleaf, P., Ahrens, L., 2022. Pilot-scale continuous foam fractionation for the removal of Per- and polyfluoroalkyl substances (PFAS) from landfill leachate. ACS ES T Water 2, 841–851.
- Soda, S., et al., 2012. Constructed wetlands for advanced treatment of wastewater with a complex matrix from a metal-processing plant: bioconcentration and translocation factors of various metals in Acorus gramineus and Cyperus alternifolius. Ecol. Eng. 39, 63–70.
- Sörengård, M., Franke, V., Tröger, R., Ahrens, L., 2020. Losses of poly- and perfluoroalkyl substances to syringe filter materials. J. Chromatogr. A 1609.
- Sörengård, M., Bergström, S., McCleaf, P., Wiberg, K., Ahrens, L., 2022. Long-distance transport of per- and polyfluoroalkyl substances (PFAS) in a Swedish drinking water aquifer. Environ. Pollut. 311.
- Stahl, T., et al., 2009. Carryover of perfluorooctanoic acid (PFOA) and perfluorooctane sulfonate (PFOS) from soil to plants. Arch. Environ. Contam. Toxicol. 57, 289–298.
- Stein, Cheryl R., McGovern, Kathleen J., Pajak, Ashley M., Maglione, Paul J., Wolff, M.S., 2016. Perfluoroalkyl and polyfluoroalkyl substances and indicators of immune function in children aged 12 – 19 years: NHANES. Pediatr. Res. 79, 348–357.
- Sunderland, E.M., et al., 2019. A review of the pathways of human exposure to poly- and perfluoroalkyl substances (PFASs) and present understanding of health effects.

 J. Expo. Sci. Environ. Epidemiol. 29, 131–147.
- Vymazal, J., 2007. Removal of nutrients in various types of constructed wetlands. Sci. Total Environ. 380, 48–65.
- Walter, J.S., Campbell, C., Kellog, E.A., Donoghue, M.J., Stevens, P., 2002. Plant Systematics: A Phylogenetic Approach, second ed.
- Wen, B., et al., 2013. Mechanistic studies of perfluorooctane sulfonate, perfluorooctanoic acid uptake by maize (Zea mays L. cv. TY2). Plant Soil 370, 345–354.
- Xiao, J., Huang, J., Wang, Y., Qian, X., 2023. The fate and behavior of perfluorooctanoic acid (PFOA) in constructed wetlands: insights into potential removal and transformation pathway. Sci. Total Environ. 861, 160309.
- Xu, J., et al., 2024. Differential uptake and translocation of perfluoroalkyl substances by vegetable roots and leaves: insight into critical influencing factors. Sci. Total Environ. 949, 175205.
- Yin, T., et al., 2017. Perfluoroalkyl and polyfluoroalkyl substances removal in a full-scale tropical constructed wetland system treating landfill leachate. Water Res. 125, 418–426.
- Zegada-Lizarazu, W., et al., 2010. Agronomic aspects of energy crops in Europe. Biofuel Bioprod. Biorefining 674–691.
- Zhang, S., Lu, X., Wang, N., Buck, R.C., 2016a. Biotransformation potential of 6:2 fluorotelomer sulfonate (6:2 FTSA) in aerobic and anaerobic sediment. Chemosphere 154, 224–230.
- Zhang, H., et al., 2016b. Uptake, translocation, and metabolism of 8:2 fluorotelomer alcohol in soybean (Glycine max L. Merrill). Environ. Sci. Technol. 50, 13309–13317.
- Zhang, D.Q., Wang, M., He, Q., Niu, X., Liang, Y., 2020. Distribution of perfluoroalkyl substances (PFASs) in aquatic plant-based systems: from soil adsorption and plant uptake to effects on microbial community. Environ. Pollut. 257, 113575.
- Zhang, W., Cao, H., Liang, Y., 2021a. Plant uptake and soil fractionation of five ether-PFAS in plant-soil systems. Sci. Total Environ. 771, 144805.
- Zhang, W., Cao, H., Liang, Y., 2021b. Degradation by hydrothermal liquefaction of fluoroalkylether compounds accumulated in cattails (Typha latifolia). J. Environ. Chem. Eng. 9.
- Zhao, S., et al., 2018. Different biotransformation behaviors of perfluorooctane sulfonamide in wheat (Triticum aestivum L.) from earthworms (Eisenia fetida). J. Hazard. Mater. 346, 191–198.
- Zhao, S., et al., 2019. Fate of 6:2 fluorotelomer sulfonic acid in pumpkin (Cucurbita maxima L.) based on hydroponic culture: uptake, translocation and biotransformation. Environ. Pollut. 252, 804–812.